

Dissipative quantum tunneling of a single defect in a disordered metal

Kookjin Chun and Norman O. Birge

*Department of Physics and Astronomy and Center for Fundamental Materials Research, Michigan State University,
East Lansing, Michigan 48824*

(Received 24 August 1995; revised manuscript received 1 March 1996)

We have studied the dynamics of single bistable defects in submicron disordered Bi wires at temperatures 0.1–2 K. The wires are sufficiently small so that the motion of a single defect can be detected as a random telegraph signal in the resistance time trace. The amplitude of the resistance jumps increases as the temperature is lowered due to the physics of universal conductance fluctuations. The defect transitions obey Poisson statistics and detailed balance, indicating that the defect is a two-state system. We interpret the signal as arising from incoherent tunneling of an atom or group of atoms between the two wells of a double-well potential. The temperature dependence of the tunneling rates agrees quantitatively with the predictions of dissipative quantum tunneling theory, which describes tunneling of a defect in the presence of strong dissipation from the electron bath. Our measurements exploit the previous discovery that the energy asymmetry ε of the defect varies with magnetic field. By varying both the temperature and magnetic field, we can probe the behavior of the tunneling rates spanning two very different regimes, from $kT \ll \varepsilon$ to $kT \gg \varepsilon$. Data from a single defect at several values of magnetic field suggest that the defect-bath coupling constant α and the renormalized tunneling matrix element Δ_r are nearly independent of magnetic field. [S0163-1829(96)05131-4]

I. INTRODUCTION

The quantum-mechanical problem of a particle tunneling in a double-well potential arises in many different contexts in physics and chemistry. An example of great historical significance is the problem of two-level tunneling systems in glasses.¹ It was proposed in the early 1970's (Ref. 2) that the presence of two-level systems (TLS's) with a broad distribution of energies and relaxation rates could account for the anomalous low-temperature thermal properties of glasses.³ TLS's arise from the presence of many nearly degenerate local minima in the potential-energy surface of the solid, due to disorder. If a pair of minima are sufficiently close in configuration space, and separated by a barrier that is not too high, then the system can move between the minima on experimentally accessible time scales. At high temperatures, the dynamics of atomic rearrangements are thermally activated over the barrier, while at low temperatures the dynamics are due to tunneling through the barrier. If the temperature is sufficiently low so that the particle is restricted to only the lowest vibrational level in each well, then the problem reduces to that of a two-level system. In disordered materials, the energies and relaxation rates of the tunneling systems are distributed over wide ranges. By making a few straightforward assumptions about the distributions of parameters describing the double-well potentials in disordered materials,² one can successfully explain the low-temperature thermal, acoustic, and dielectric properties of glasses.¹

The original "tunneling model" described above was very successful at describing the low-temperature properties of insulating glasses; however, it was less successful when applied to metallic glasses.^{4,5} Another difficulty with the model is that, until quite recently, there was no direct evidence of the individual tunneling entities—all the predictions were based on the statistical properties of the ensemble of TLS's. This latter difficulty, although more philosophical

than practical, would nevertheless be eliminated if one were able to measure the properties of an individual tunneling system in a very small sample of disordered material.

The development of submicrometer fabrication techniques over the past decade gives us a tool to address the issues described above. Now one can routinely fabricate samples of sufficiently small size such that there are only a few tunneling systems within an experimentally determined energy range and bandwidth. (For a disordered sample of dimensions $1 \times 0.1 \times 0.01 \mu\text{m}^3$, one expects on the order of ten TLS's within an energy range of 1 K and a bandwidth of several decades of time or frequency.⁶) With samples of such small size, one is not able to perform the traditional measurements of TLS's, such as specific heat, thermal conductivity, or sound propagation and absorption. One can, however, measure the electrical resistance of such small samples quite readily. In fact, we will show below that the electrical resistance of small samples at low temperature is quite sensitive to the motion of individual atoms, due to the physics of universal conductance fluctuations.^{7–10} This suggests a powerful technique for studying the physical behavior of individual TLS's within electrically conducting samples of submicrometer dimensions.

Several groups have studied the motion of individual defects in metals.^{11–15} Experiments performed by Golding, Zimmerman, and Coppersmith¹⁴ and by us¹⁵ focus on the tunneling dynamics of defects, at temperatures down to 0.1 K.¹⁵ We restrict ourselves to TLS's that are observable in the time trace of the electrical resistance, i.e. those that undergo slow, incoherent tunneling. (Fast TLS's are not observable in the time domain, but they give rise instead to anomalies in the I - V characteristic of ultrasmall samples.¹⁶) The outline of the paper is as follows: first we outline the theoretical understanding of tunneling systems interacting with the conduction electrons in metals, then we summarize the theory of universal conductance fluctuations necessary to understand

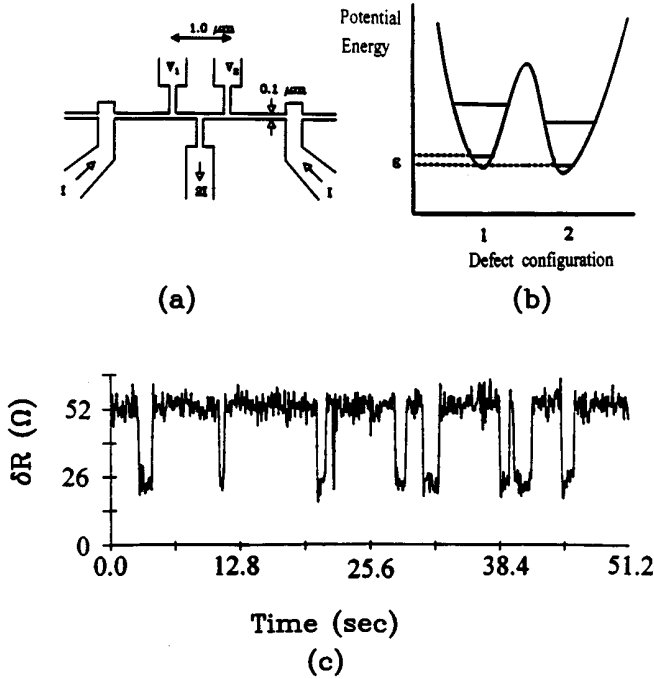


FIG. 1. (a) Schematic diagram of the sample with five leads. (b) Schematic diagram of a double-well potential. At low temperatures ($kT < \hbar\omega_0$), the dynamics are dominated by tunneling between the ground states in each well. (c) Resistance change δR as a function of time, at $B=6.997$ T and $T=0.132$ K. The resistance switches between two values, corresponding to the tunneling of the single defect between two states. The resistance of each arm of the sample is about 1 K Ω , and δR in this case is about 30 Ω .

our experiments. We then present our measurements of a single tunneling defect in a Bi wire, over a wide range of both temperature and magnetic field. We compare the data with theory, and discuss the magnetic-field dependence of the parameters of the theory. A preliminary discussion of this work has already appeared.¹⁵

Experimental measurements of dissipative tunneling have also been carried out in crystalline metals.¹⁷⁻¹⁹ Those studies are limited to the special case of the symmetric multiwell potential, whereas the defect potentials in our disordered samples have no symmetry constraint.

II. DISSIPATIVE QUANTUM TUNNELING THEORY

The TLS model describes a defect in a double-well potential at sufficiently low temperature so that the excited energy levels of the system are inaccessible, and the dynamics of a particle only involves the tunneling back and forth between the lowest states of each potential well. Figure 1(b) shows a schematic diagram of a double-well potential. For an isolated tunneling system, the Hamiltonian for a single defect moving in an asymmetric double-well potential is $H_0 = (\varepsilon/2)\sigma_z - (\hbar\Delta_0/2)\sigma_x$, where σ_i are Pauli spin matrices, ε is the energy asymmetry, and Δ_0 is the bare tunneling matrix element, given by the WKB approximation in one dimension as $\Delta_0 = \omega_0 \exp[-\sqrt{(2mV_0/\hbar^2)}\delta r]$. The tunneling dynamics for this Hamiltonian are coherent, with energy eigenstates that are linear combinations of the states in each well.

In a metal, the defect interacts strongly with the bath of

conduction electrons, resulting in Ohmic dissipation of the tunneling system. When the temperature is much greater than the tunneling matrix element, dissipative tunneling shows the following features:²⁰⁻²² (1) incoherent tunneling of the defect, arising from the continuous dephasing of the defect wavefunction by interactions with the electron bath; (2) renormalization of the bare tunneling matrix element due to interaction of the defect with the high-energy (adiabatic) electron-hole excitations; and (3) a striking temperature dependence of the tunneling rates—for $kT > \varepsilon$, the rates increase with decreasing temperature, following a power law $\gamma_f, \gamma_s \sim T^{2\alpha-1}$,²³ with $0 < \alpha < 1/2$ for metals.²⁴

The theoretical approach to the dissipative quantum tunneling problem proceeds as follows:²⁰ if the barrier height between the two wells is much larger than the small undamped oscillation frequency ω_0 in either well, then the bare tunneling rate Δ_0 satisfies $\Delta_0 \ll \omega_0$. If, in addition, $kT \ll \hbar\omega_0$, then the double-well problem can be reduced to an effective, biased two-level system. The bath of electron-hole excitations can be separated into two classes, which play two quite different roles. The electron-hole excitations of frequency greater than a cutoff frequency ω_c are able to follow the tunneling defect adiabatically.²⁵ Here ω_c is a theoretical quantity introduced in the course of reduction to a TLS, and is assumed to be $\Delta_0 \ll \omega_c < \omega_0$. This leads to a renormalization of the tunneling matrix element Δ through the relation

$$\Delta = \Delta_0 (\omega_c / \omega_0)^\alpha. \quad (1)$$

The remaining electron-hole excitations with frequency smaller than ω_c cannot follow the defect adiabatically; they are directed toward the center of the well.²⁵ This nonadiabatic character of the bath has a striking effect on the tunneling dynamics, as we show below. The assumption of the system being reduced to an effective TLS and the incorporation of the high-energy electron-hole excitations into a renormalized matrix element give rise to a truncated Hamiltonian, given by

$$H = \frac{\varepsilon}{2} \sigma_z - \frac{\hbar\Delta}{2} \sigma_x + \sigma_z \sum_j G_j (b_j + b_j^\dagger) + \sum_j \hbar\omega_j b_j^\dagger b_j. \quad (2)$$

Caldiera and Leggett²⁶ showed that the influence of the low-energy electron-hole excitations on the tunneling defect can be modeled by a bath of harmonic oscillators. The third term describes the interaction between the defect and the bath, where b_j^\dagger and b_j are creation and annihilation operators of the harmonic oscillators, and G_j are coupling coefficients between the defect and the harmonic oscillators. The fourth term is the Hamiltonian of the harmonic-oscillator bath itself.

The effect of the bath on the defect dynamics depends only on the spectral density of the bath excitations, $J(\omega) = (2/\hbar^2) \sum_j G_j^2 \delta(\omega - \omega_j)$. For a metal, the spectral density in the continuum limit takes the form $J(\omega) = \alpha\omega$ for $\omega < \omega_c$.²⁷ The coupling of the defect to the bath is characterized in terms of the single parameter α .

If the Hamiltonian of Eq. (2) is to represent faithfully the dynamics of a particle double-well potential, then its solution must not depend on the arbitrary choice of the cutoff fre-

quency ω_c , that enters into Eq. (1).²⁰ In fact, the tunneling rate calculated from Eq. (2) depends only on a new renormalized rate Δ_r , defined as

$$\Delta_r = \Delta (\Delta / \omega_c)^{\alpha/(1-\alpha)} = \Delta_0 (\Delta_0 / \omega_0)^{\alpha/(1-\alpha)}, \quad (3)$$

where the second equality makes use of Eq. (1). Note that ω_c does indeed drop out of the final result.

When $\hbar\Delta_r \ll \varepsilon$, αkT , the coupling of the defect to the bath is so strong that the fluctuations of the bath break the phase coherence of the tunneling defect, and the tunneling becomes incoherent.²⁰ The dynamics of the tunneling transitions are characterized by the occupation probability of the defect $P(t) = \langle \sigma_z(t) \rangle$, given that for $t < 0$ the particle is localized in the $\sigma_z = +1$ state. For a double-well potential with energy asymmetry ε , one finds $P(t) = -\tanh(\varepsilon/2kT) + [1 + \tanh(\varepsilon/2kT)]e^{-\gamma}$, with a tunneling rate²⁰⁻²² of

$$\gamma = \frac{\Delta_r}{2} \left(\frac{2\pi kT}{\hbar\Delta_r} \right)^{2\alpha-1} \frac{\cosh\left(\frac{\varepsilon}{2kT}\right)}{\Gamma(2\alpha)} \left| \Gamma\left(\alpha + i\frac{\varepsilon}{2\pi kT}\right) \right|^2, \quad (4)$$

where $\Gamma(x+iy)$ is the complex γ function. The above equation describes incoherent relaxation with a transition rate γ . For a single TLS, the energy asymmetry ε is related to the ratio of the average time spent in each state, averaged over many transitions. This must obey the principle of detailed balance $\gamma_f/\gamma_s = e^{\varepsilon/kT}$, where γ_f and γ_s are the fast and slow transition rates, i.e., the reciprocals of the lifetimes of the excited or ground states, respectively. The total rate equals the sum of the fast and slow rates, $\gamma = \gamma_f + \gamma_s$. From detailed balance, we finally have

$$\gamma_f = \frac{\Delta_r}{4} \left(\frac{2\pi kT}{\hbar\Delta_r} \right)^{2\alpha-1} \frac{e^{\varepsilon/2kT}}{\Gamma(2\alpha)} \left| \Gamma\left(\alpha + i\frac{\varepsilon}{2\pi kT}\right) \right|^2$$

and $\gamma_s = \gamma_f e^{-\varepsilon/kT}$. (5)

For $0 < \alpha < 1/2$, there are two regimes depending on the relative magnitude of kT and ε . When $kT > \varepsilon$, the tunneling rates increase with decreasing temperature, $\gamma_f, \gamma_s \sim T^{2\alpha-1}$,²³ which is a striking feature of dissipative quantum tunneling. When $kT < \varepsilon$, the tunneling rates follow a simple picture of stimulated absorption and spontaneous emission. The fast rate γ_f is determined by the sum of the spontaneous and stimulated emission rates, while the slow rate is determined by the stimulated absorption rate. As temperature is lowered, the fast rate is roughly temperature independent, and the slow rate decreases rapidly as $e^{-\varepsilon/kT}$.

III. QUANTUM TRANSPORT

Our interest in dissipative quantum tunneling arose from the problem of tunneling systems in disordered materials, as described in Sec. I. Since the parameters describing the tunneling systems (barrier asymmetry, tunneling matrix element) are widely distributed in disordered materials, we require a measurement technique that allows us to measure the properties of a single tunneling system. Fortunately we have such a tool, in the electrical resistance of a metal wire with submicrometer dimensions. It is not obvious, however, that

we can detect the motion of a single TLS in a metal wire at low temperature. Although we can limit the number of active TLS's in a sample by shrinking the sample size, detection of a TLS via the electrical resistance requires passing a current through the sample, which necessarily entails Ohmic heating of the conduction electrons. The problem of electron heating becomes increasingly severe as sample size decreases and temperature is lowered, due to the shrinking electronic heat capacity and the rapidly decreasing electron-phonon scattering rate. As a result, the applied current, and hence the measured voltage, must be decreased rapidly as the temperature is lowered.

As it turns out, nature has been kind to us; the sensitivity of the electrical resistance to the motion of an atomic defect *increases* as the temperature is lowered,^{9,10} due to the physics of universal conductance fluctuations, or UCF.^{7,8} Although the increase is not large enough to offset the decrease in signal that follows from the lower drive necessary to avoid electron heating, it is nevertheless large enough to allow the measurements described here to be performed at temperatures as low as 0.1 K.

The physics of UCF arises from quantum interference of multiply scattered conduction electrons due to disorder. UCF theory is valid whenever the phase-breaking rate for conduction electrons (due to inelastic or spin-flip scattering, for example) is much less than the elastic scattering rate from the disorder. In this regime the motion of the charge carriers is diffusive, with diffusion constant $D = \frac{1}{3}\nu_F l_e$, where ν_F is the Fermi velocity and l_e is the elastic mean free path. Electron transport is diffusive in polycrystalline metals below several tens of K, and in amorphous metals up to room temperature. In the diffusive regime, the distance over which conduction electrons maintain phase coherence is $L_\phi = \sqrt{D\tau_\phi}$, which is typically of order one micrometer at a temperature of 1 K. The electrical conductance on a length scale less than L_ϕ cannot be derived simply by adding independently the scattering rates from all the scattering centers, but rather the conductance is given by the coherent sum of the amplitudes of multiply scattered waves from different trajectories.

The consequences of quantum interference are quite apparent in mesoscopic samples, i.e., samples with dimensions comparable to L_ϕ .⁷ The conductance of such samples is sensitive not only to the details of the atomic disorder potential, but also to the application of a magnetic field. The magnetic field changes the relative phases of different electron trajectories through the sample, hence it changes the interference pattern and thus the sample conductance. Traces of conductance versus magnetic field show a random, static pattern of fluctuations, called the ‘‘magnetofingerprint.’’ The amplitude of the conductance fluctuations are of order e^2/h , hence the name universal conductance fluctuations.⁸

Another way to observe universal conductance fluctuations in a mesoscopic sample is to change the locations of the scattering centers, i.e., the impurities and defects.^{9,10} If a scatterer moves, it changes the phases of all the paths that scatter from it, resulting in a conductance change. For a disordered metal in the diffusive regime, multiple elastic scattering is very much like a random walk process with a step size l_e . In quasi-one-dimensional systems, a typical electron trajectory passes through a given site many times; therefore

the motion of a single scatterer can affect all the scattered paths and accumulate sufficient phase shift to change the conductance by the full amount $\delta G \approx e^2/h$, as much as if all the scatterers are moved around. The average conductance change of a quasi one-dimensional (1D) wire due to the motion of a single scatterer for $l_e \ll L_x \approx L_y \ll L_z < L_\phi$, where L_x , L_y , and L_z are thickness, width, and length, respectively,¹⁰ is

$$(\delta G_1)^2 = C \left(\frac{e^2}{h} \right)^2 \frac{1}{(k_F l_e)^2} \alpha(k_F \delta r) \frac{l_e L_z}{L_x L_y}. \quad (6)$$

Here C is a constant of order unity, and the function $\alpha(x) = 1 - \sin^2(x/2)/(x/2)^2$ accounts for the phase shift due to moving a scatterer a distance δr .

At finite temperature, the magnitude of the conductance fluctuations is reduced due to the effect called ‘‘energy averaging.’’ When $kT > \hbar \tau_\phi^{-1}$, the conductance fluctuations are reduced in magnitude due to averaging over $kT/\hbar \tau_\phi^{-1}$ uncorrelated patterns. The expression for $(\delta G)^2$ is thus multiplied by the factor $\hbar \tau_\phi^{-1}/kT = L_T^2/L_\phi^2$, where $L_T = \sqrt{\hbar D/kT}$ is the thermal length.

IV. EXPERIMENTAL MEASUREMENT AND ANALYSIS

Our samples are polycrystalline Bi wires 20 nm thick, prepared by thermal evaporation at room temperature onto oxidized Si substrates at a pressure of about 1×10^{-6} Torr. The wires were patterned using electron-beam lithography into five-terminal devices for use in a Wheatstone bridge. The two arms of the sample have nominally identical sample regions with areas of $5 \times 10^{-2} \mu\text{m}^2$ (a linewidth of 0.1 μm and a length of 0.5 μm). Figure 1(a) shows the configuration of a sample and its leads. Each arm of the sample has a resistance of about 1 k Ω . The difference of the resistances of the two arms is measured using an ac source and a lock-in amplifier at a few hundred Hz.

We have measured the electrical conductance of several Bi wires in the five-terminal configuration. All samples show signs of individual defects at temperatures below 1 K. The signature of a single defect is a random telegraph signal, such as that shown in Fig. 1(c), in the time trace of the differential resistance of the bridge. The resistance jumps δR across the bridge are due to the motion of a single defect in either arm of the sample. In this paper we focus on data from a single sample where we found very clean signals from a particular defect. This defect not only gave rise to a relatively large value of δR , but the jump rate was relatively slow ($\sim 1 \text{ s}^{-1}$), allowing us to limit our experimental bandwidth and thereby limit the background noise due to the preamplifier and to other, faster, defects. In addition, the defect was extremely stable—the data reported here were accumulated over a period of two months. We note that this defect is typical of many defects we have observed in Bi samples; the data reported here are unusual only in the sense that the signal-to-noise ratio was the best we have achieved to date; hence we were able to obtain measurements of the transition rates over a very broad temperature range (see below).

The magnitude of the conductance jumps due to the defect motion increases with decreasing temperature, due to the

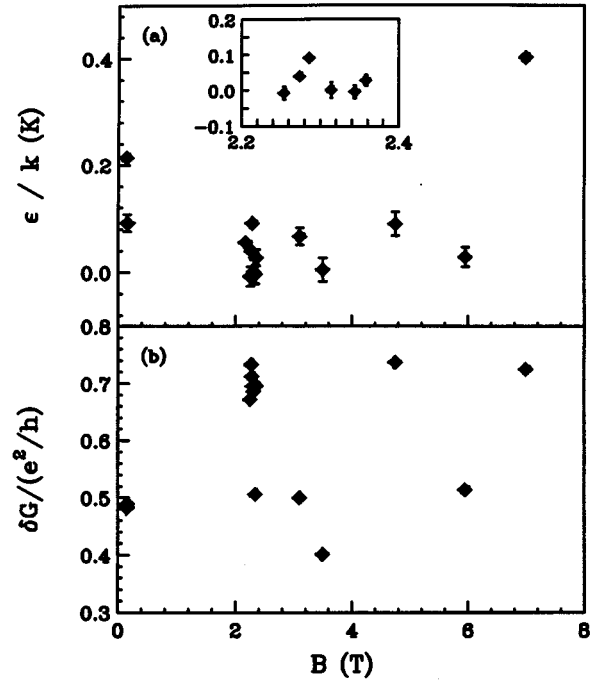


FIG. 2. (a) Energy asymmetry ε vs magnetic field for a single defect. The data points with the small uncertainties were obtained from fits to the detailed balance relation (Ref. 15); the other values were determined from data taken at a single temperature. (b) Conductance change δG vs magnetic field at $T = 0.3$ K. The plot shows only those values of magnetic field where the conductance signal due to the motion of a single defect was maximum. The inset in (a) shows ε over a narrow range of B , where we attempted (but failed) to determine if ε changes sign. The relative sign of ε and of δG cannot be determined for data sets far apart in B , since either quantity may change sign in a region of magnetic field where the defect signal is not observable.

increase in the phase-breaking length, L_ϕ , in the sample. For this defect, the jumps in conductance ($\delta G = \delta R/R^2$) were of order 0.2 e^2/h at 1 K and 1.0 e^2/h at 0.1 K ($e^2/h \approx 4 \times 10^{-5} \Omega^{-1}$). Even in this sample, however, one does not observe time traces like that shown in Fig. 1(c) under all circumstances. Just as the conductance of the sample depends on magnetic field in a random way (the ‘‘magnetofingerprint’’ mentioned earlier), so the conductance jump δG due to a particular defect also varies with magnetic field in a random way. Figure 2(b) illustrates this random variation of δG with respect to the applied magnetic field, for one defect at a temperature of 0.3 K. In the figure, the absolute value of δG is shown only where it is significantly larger than the background noise of the measurement. At other values of the magnetic field, the signal due to this defect was masked either by preamplifier noise or by conductance jumps from other defects.

The data presented in this paper were obtained at those values of magnetic field shown in Fig. 2(b), where the conductance signal δG has its maximum value, and where the total noise from other defects was much smaller. Magnetic fields where we observed mixed signals from several defects were not used for analysis. We found five different magnetic fields where the signal for a single fluctuator was particularly

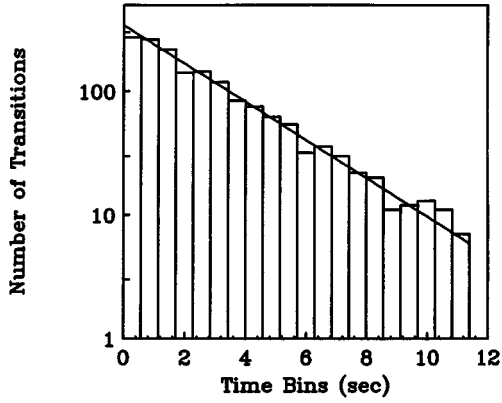


FIG. 3. The dwell times in each state are histogrammed and fit to a single-exponential decay function to find the mean transition time, τ , and the tunneling rate to the other state, $\gamma = \tau^{-1}$.

clean: $B = 0.140, 2.170, 2.274, 2.286,$ and 6.997 T. At each of these magnetic fields, we measured the transition rates of the defect as a function of temperature. For good statistics, several hundred transitions of the defect were recorded and analyzed at each temperature.

It is not obvious *a priori* that the data sets taken at the five values of magnetic field listed above arise from the same defect. In fact, we were able to follow the defect signal nearly continuously as a function of field from 0 to 3 T, but there were vast ranges between 3 and 7 T where no defect signal was visible. Fortunately, as we will show below, the data set at 7 T can be described with the same values of the fitting parameters (most importantly the renormalized tunneling matrix element) as the other data sets. Given that the tunneling matrix element is essentially a random variable for defects in disordered materials, we therefore have strong *a posteriori* evidence that the 7-T data arise from the same defect as the other data sets.

Our measurements were limited to temperatures between 0.1 and 2.0 K. Above 2.0 K, several defects became very active, so it was difficult to follow the dynamics of a particular defect at any magnetic field. Below 0.1 K the signal-to-noise ratio was very small. Although δG increases as the temperature is lowered, the drive current must be decreased even faster to avoid sample heating.²⁸ We used a drive current of 0.7 nA at 0.1 K. The conductance (measured as the voltage at the output of the lock-in amplifier) was low-pass filtered, then sampled by the computer at a sampling frequency of 20 or 50 Hz, depending on the fast tunneling rate γ_f of the defect.

Raw data of voltage versus time were analyzed using two independent methods. With the first method we set two comparator levels to locate the transitions between the two states, and then we measure the dwell times in each state. Figure 3 shows a histogram of dwell times in one of the states at $B = 6.997$ T and $T = 0.132$ K as a result of the analysis. The straight line is a fit to an exponential, $N(t) = N_0(e^{-t/\tau} - e^{-(t+\Delta t)/\tau})$, where Δt is the bin size. The fit determines the mean dwell time in that state τ , and shows that the dwell times follow a Poisson distribution. The tunneling rate to the other state γ is then obtained from the

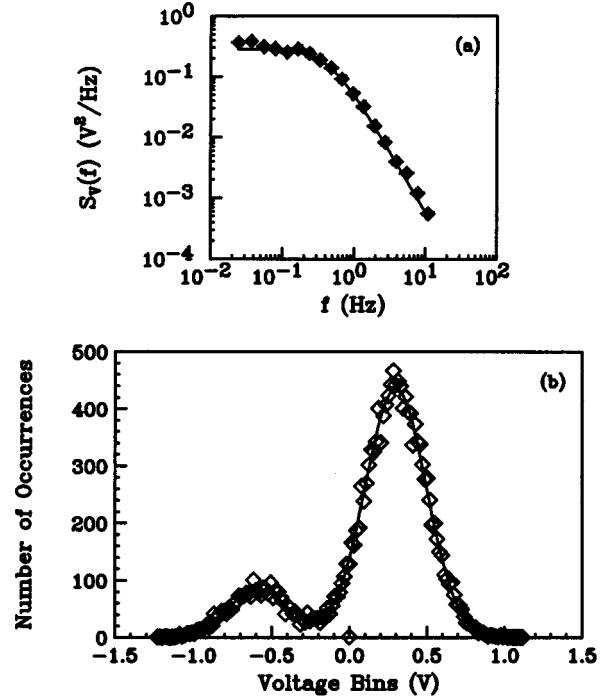


FIG. 4. (a) The power spectrum of the time trace data. The spectrum is fit with a Debye-Lorentzian function to determine the sum of the transition rates for the two-level system. (b) Histogram of raw values of resistance. The solid line is a fit to the sum of two Gaussians. The ratio of the areas of the two Gaussians determines the ratio of the two transition rates.

relation $\gamma = \tau^{-1}$. In general the two tunneling rates are unequal; we call the fast and slow rates γ_f and γ_s , respectively.

The second analysis method uses a combination of two different fitting procedures; we fit the power spectrum of the voltage time trace (after background subtraction) to a Debye-Lorentzian line shape²⁹ to find the sum of the two tunneling rates, $\gamma = \gamma_f + \gamma_s$, and we fit the histogram of the raw voltage values to the sum of two Gaussians to obtain the ratio of the rates, γ_f/γ_s . Figure 4(a) shows a fit of a power spectrum to a Debye-Lorentzian function. The power spectral density $S_V(f)$ for the single defect was obtained over the frequency range 10^{-2} –10 Hz, using a fast Fourier transform of the raw voltage data.

We expect the voltage values in each state to have a Gaussian distribution with standard deviation σ , due to thermal and preamplifier noise. Since the voltage jump due to the motion of a defect is given as $dV = V_2 - V_1$, the overall distribution of raw voltage values should be the sum of two independent Gaussians centered at peak values, V_1 and V_2 . Figure 4(b) illustrates the fit of a histogram of the raw voltage values to the sum of two Gaussians. The fit gives the areas and peak values of each Gaussian. The ratio of the two areas is the ratio of the dwell times, and hence the transition rates γ_f/γ_s . There is good agreement between the data and the fit. The value of γ obtained from the fit to the power spectrum and the value of the ratio γ_f/γ_s from the two-Gaussian fit, together determine both γ_f and γ_s . The results

of this analysis are in good agreement with those obtained from the first analysis method.

The exponential distribution of dwell times in each state of the fluctuator suggests that the data correspond to a two-level system in the sample. We also expect the transition rates to obey the principle of detailed balance, $\gamma_f/\gamma_s = e^{\varepsilon/kT}$, where ε is the energy asymmetry of the defect potential. Plots of $\ln(\gamma_f/\gamma_s)$ versus $1/T$ for the data taken at four different values of magnetic field are shown in Fig. 2 of Ref. 15. The excellent linear fits through the origin confirm the above relation. The slopes of the lines for $B = 6.997, 0.140, 2.286,$ and 2.274 T gives values for ε/k_B of 402, 213, 92, and 40 mK, respectively, with a standard deviation less than 10 mK.

Figure 2(a) shows the absolute value of ε versus magnetic field for this defect. (We cannot determine the relative sign of ε between data sets widely spaced in field, since the sign of δG varies randomly with field.) The five data points with small uncertainties were obtained from the fits in Ref. 15, plus an additional fit at $B=2.170$ T. The other values of ε were obtained from measurements at a single temperature, 0.24 K. Figure 2(a) shows that ε varies randomly with B . A random variation of ε with B in a disordered sample was predicted by Al'tshuler and Spivak,³⁰ and first observed experimentally by Zimmerman, Golding, and Haemmerle.¹⁴ The energy asymmetry of the defect is determined in part by the local-electron charge density at the defect site, which fluctuates spatially due to the Friedel oscillations caused by the neighboring scattering centers.³¹ Application of a magnetic field alters the interference pattern of the Friedel oscillations, and thereby changes the local charge density. The theory predicts that ε can either increase or decrease with B .³² By chance, the three defects studied by Zimmerman and co-workers¹⁴ all showed an increase in ε with B . Our data show that ε for this particular defect decreases with B (near $B=0$), so there is no need to postulate an *ad hoc* correlation between the bare value of ε and the effect of magnetic field.³²

The magnetic-field scale characterizing the variation of ε is determined by the magnetic length, $L_B = \sqrt{\hbar/eB}$. (This is in contrast to the case of the conductance itself, which fluctuates randomly with magnetic field with a scale determined by the phase-breaking length L_ϕ .) The order of magnitude of the expected change in ε with field is given by^{30,32}

$$\begin{aligned} \langle [\varepsilon(B) - \varepsilon(0)]^2 \rangle &= \frac{\ln 2 \alpha E_B^2}{6 \pi \hbar D \nu(0)} \approx \alpha (\hbar \omega_c)^2 \frac{l_e}{L_x} \\ &\approx (k_B 0.3KB)^2, \end{aligned} \quad (7)$$

where $E_B = 2DeB$, D is the carrier diffusion constant, $\nu(0)$ is the effective 2D density of states at the Fermi level, and L_x is the sample thickness.³³ To obtain the final estimate, where B is in T, we plugged in the values for our Bi sample: $l = 5$ nm and $L_x = 20$ nm, and we used the free-electron mass in ω_c . According to this estimate, typical fluctuations in ε/k_B over a magnetic field range of 7 T are of order 2 K. Hence the observed variation of ε/k_B for our defect is somewhat smaller than typical.

One of the goals of this work is to compare our experimental measurement of the defect tunneling rates with the

predictions of dissipative quantum tunneling theory. In particular, we wish to test the theory over a temperature range spanning the two limiting cases, $kT \ll \varepsilon$ and $kT \gg \varepsilon$. In our experiment we were able to measure defect transitions over the temperature range 0.1–2.0 K. This factor of 20 in temperature is substantial, but would not be entirely adequate for our purpose if ε were fixed at a single value for each defect studied. Hence the variation of ε with field discussed above is quite fortuitous. Figure 5, which is the central result of this work, shows how the rates for the defect vary with temperature at the five different values of magnetic field we studied in depth. The data show clearly the different temperature regimes of dissipative quantum tunneling. At $B=0.140$ T, with $\varepsilon/k_B = 213$ mK, the data most clearly illustrate three distinct temperature regimes. When $kT < \varepsilon$, γ_f is roughly temperature independent, while γ_s decreases rapidly with decreasing temperature. This behavior is in accord with the picture of spontaneous emission and stimulated absorption. As the temperature is raised so that $kT > \varepsilon$, the rates cross over to a qualitatively different regime. The ratio of the two rates still obeys detailed balance, but both rates *decrease* with increasing temperature. At $B=2.274, 2.170,$ and 2.286 T, where most of the data are in the regime $kT > \varepsilon$, it is shown more vividly that the temperature dependence of the rates follows a power law, $T^{2\alpha-1}$. This behavior is one of the essential features of dissipative quantum tunneling in metals. Above 1.2 K, the rates increase rapidly for all values of magnetic field, due first to phonon-assisted tunneling, and eventually to thermal activation over the barrier.

The theory of dissipative quantum tunneling discussed earlier describes the tunneling of a particle between only two states in the presence of conduction electrons, and does not describe the rapid increase of the rates above 1.2 K. We believe that the rapid increase arises from thermal excitation to the first excited vibrational state in each well, followed by rapid tunneling through the reduced barrier.³⁴ (An alternative proposed mechanism involves coupling of the two-state system to phonons.³⁵) The rate increase is not included in the theoretical result of Eq. (5), hence we limit quantitative analysis here to the temperature range below 1.2 K. The temperature dependence of the tunneling rates γ_f and γ_s was fit to Eq. (5), with α and Δ_r as free parameters. (The value of the energy asymmetry ε was fixed by the results of the detailed balance fits discussed earlier. The dotted lines in Fig. 5 are the two-parameter least-square fits, which show excellent agreement with the data at all temperatures below 1.2 K. The parameter values are consistent with the dissipative tunneling model in the limit of incoherent tunneling, i.e., $\hbar\Delta_r \ll \varepsilon$, αkT , and $0 < \alpha < \frac{1}{2}$.)

The least-square fits appear to indicate that α and Δ_r vary with magnetic field. We have found, however, that the quality of the fits are rather insensitive to a specific correlated change of α and Δ_r . This can be seen in Fig. 6, which shows the values of α and Δ_r determined from the five fits. The values of α and Δ_r from the fits are highly correlated, and fall on a straight line when plotted as $\ln(\Delta_r)$ vs $\alpha/1-\alpha$. In fact, the χ^2 for any one of the fits changes very slowly when α and Δ_r move along the straight line connecting the five points in the figure. This suggests that all five data sets can

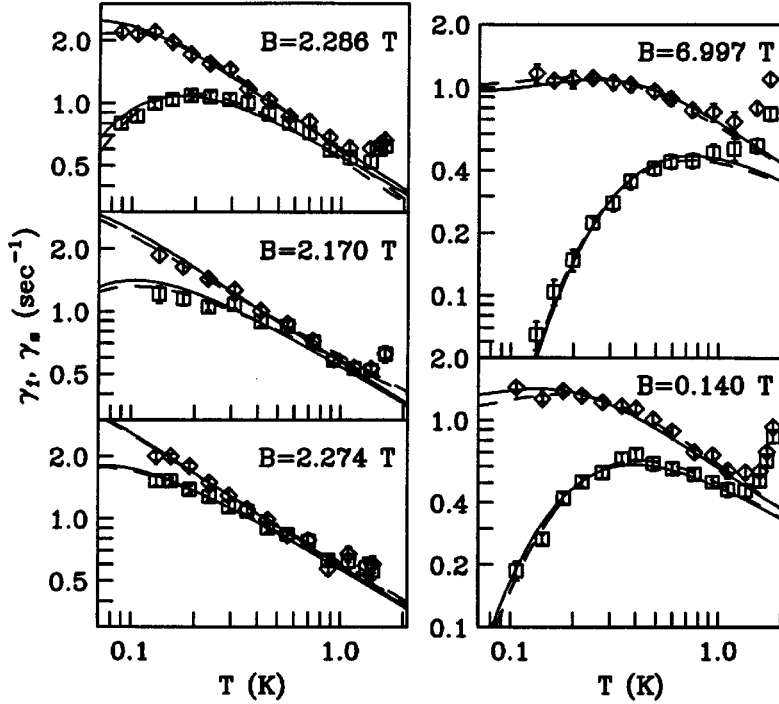


FIG. 5. Fast and slow transition rates vs temperature, for five values of the applied magnetic field. Dashed lines are two-parameter fits of Eq. (5) to the data for $T < 1.2$ K. The values of ε/k are fixed by the fits shown in Fig. 2 of Ref. 15. They are 402 and 213 mK (right), and 92, 73, and 40 mK (left), from top to bottom. The values of α from the fits are 0.22 and 0.16 (right), and 0.14, 0.24, and 0.21 (left), respectively, with an uncertainty of ± 0.01 . Solid lines are global fits to all five data sets with the single value of $\alpha = 0.195$, as discussed in the text.

be fit with a unique set of parameters α and Δ_r . When we perform such a global fit, we find that we are left with residuals that indicate a slight systematic shift in the overall tunneling rate as a function of magnetic field. The data for $B = 6.997$ T, in particular, require a slightly higher value of Δ_r than the other data sets. So, instead, we have chosen to fit all the data with a single value of the parameter α , while letting Δ_r vary between sets. The solid lines in Fig. 5 represent the results of that global fit. The global minimum of χ^2 was achieved with the value $\alpha = 0.195$, and with Δ_r varying only slightly with magnetic field. The data are clearly consistent with a single value of α that is independent of magnetic field for this defect.

Figure 7 shows the dependence of Δ_r on magnetic field, obtained from the global fits to the data with $\alpha = 0.195$. As discussed earlier, the local-electron density $n(B)$, and hence the density of electron-hole excitations near the defect, is

sensitive to magnetic field. This results in a modification of the polaron effect due to the nonadiabatic excitations that do not follow the defect when it tunnels. It is plausible that the modification of the polaron effect gives rise to the observed magnetic-field dependence of the tunneling matrix element Δ_r .³²

V. CONCLUSIONS

We have measured the tunneling rates of single defects in submicron Bi wire over a broad range of temperature and magnetic field. Our data for a particular defect, over the temperature range from 0.1 to 2 K, allow us to make a thorough comparison between experiment and theory. Below 1.2 K, the temperature dependence of the tunneling rates agrees quantitatively with predictions of dissipative quantum tunneling theory, spanning the regimes from $kT \ll \varepsilon$ to $kT \gg \varepsilon$.

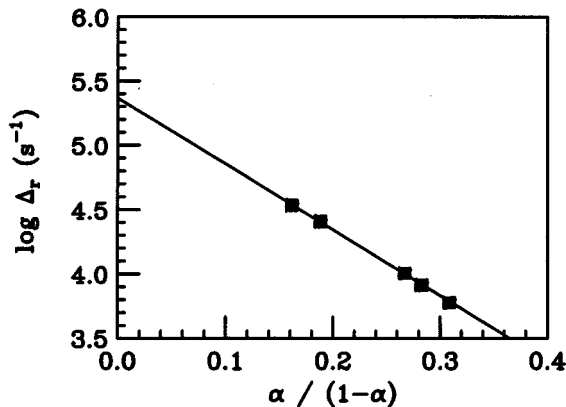


FIG. 6. Plot of Δ_r vs $\alpha/(1-\alpha)$ given from the five two-parameter fits shown in Fig. 5.

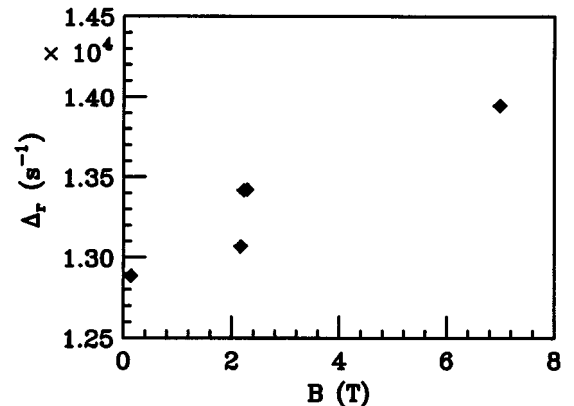


FIG. 7. Plot of Δ_r vs magnetic field. The values of Δ_r are obtained from the global fits (solid lines in Fig. 5) with $\alpha = 0.195$.

In agreement with previous work,¹⁴ we observe a random variation of ε , with magnetic field, but unlike the defects studied previously, the minimum value of ε for this defect occurs for $B \neq 0$. Our data are consistent with the hypothesis that the defect-electron bath coupling constant α is independent of magnetic field.

It is worthwhile to ask whether the defects observed in these experiments are a generic feature of disordered materials, or whether they are particular to polycrystalline Bi samples. There is much evidence to suggest that they are generic. First, other workers have observed discrete conductance fluctuations at low temperature in other disordered materials.^{11,12} Although those studies did not encompass measurements of tunneling rates below 1 K, they did establish the existence of discrete fluctuators in a wide variety of disordered metals. Second, we know that Bi samples larger than (but otherwise similar to) those studied here, exhibit low-frequency $1/f$ noise in their conductance at temperatures as low as 0.3 K, due presumably to a superposition of fluctuators of the type reported here.³⁶

We have observed similar $1/f$ noise in Ag and Li samples,³⁷ and we have no reason to believe that other disordered metals would behave differently. Finally, low-temperature studies of metals using probes other than the conductance have shown that tunneling systems are a ubiquitous feature of disordered materials, and that the density of the TLS's is rather insensitive to the nature or degree of the disorder.³⁸

ACKNOWLEDGMENTS

We have benefited from helpful discussions with many people, including G. Alers, S. Coppersmith, R. Cukier, B. Golding, A. Leggett, P. McConville, J.-S. Moon, M. Weissman, A. Zawadowski, and N. Zimmerman. In addition, we thank M. Dubson for the use of his lithographic facilities, and W. Pratt, Jr. for his thermometer calibration. This work was supported in part by the National Science Foundation under Grant No. DMR-9321850.

-
- ¹See W. A. Phillips, in *Amorphous Solids, Low-Temperature Properties*, edited by W. A. Phillips (Springer-Verlag, New York, 1981); W. A. Phillips, *Rep. Prog. Phys.* **50**, 1659 (1987), and references therein.
- ²P. W. Anderson, B. I. Halperin, and C. M. Varma, *Philos. Mag.* **25**, 1 (1972); W. A. Phillips, *J. Low Temp. Phys.* **7**, 351 (1972).
- ³R. C. Zeller and R. O. Pohl, *Phys. Rev. B* **4**, 2029 (1971).
- ⁴J. L. Black, in *Glassy Metals I*, edited by H.-J. Guntherodt and H. Beck (Springer-Verlag, New York, 1981).
- ⁵The results of dissipative quantum tunneling theory have recently been applied to metallic glasses by S. N. Coppersmith and B. Golding, *Phys. Rev. B* **47**, 4922 (1993).
- ⁶A typical density of tunneling centers in amorphous materials is given in Refs. 1 or 4 as $P \approx 10^{44} \text{ J}^{-1} \text{ m}^{-3}$. P should be multiplied by the temperature, the sample volume, and a bandwidth factor $\ln(t_{\max}/t_{\min})$, to obtain the density of tunneling centers observed in an experiment.
- ⁷C. P. Umbach, S. Washburn, R. B. Laibowitz, and R. A. Webb, *Phys. Rev. B* **30**, 4048 (1984). For a review of the experimental literature, see *Mesoscopic Phenomena in Solids*, edited by B. L. Al'tshuler, P. A. Lee, and R. A. Webb (North-Holland, New York, 1991).
- ⁸A. D. Stone, *Phys. Rev. Lett.* **54**, 2692 (1985); P. A. Lee and A. D. Stone, *ibid.* **55**, 1622 (1985); B. L. Al'tshuler, *Pis'ma Zh. Éksp. Teor. Fiz.* **41**, 530 (1985) [*JETP Lett.* **41**, 648 (1985)]. A thorough discussion of UCF theory is given in P. A. Lee, A. D. Stone, and H. Fukuyama, *Phys. Rev. B* **35**, 1039 (1987).
- ⁹B. L. Al'tshuler and B. Z. Spivak, *Pis'ma Zh. Éksp. Teor. Fiz.* **42**, 363 (1985) [*JETP Lett.* **42**, 447 (1985)].
- ¹⁰S. Feng, P. A. Lee, and A. D. Stone, *Phys. Rev. Lett.* **56**, 1960 (1986); **56**, 2772(E) (1986).
- ¹¹D. E. Beutler, T. L. Meisenheimer and N. Giordano, *Phys. Rev. Lett.* **58**, 1240 (1987); T. L. Meisenheimer and N. Giordano, *Phys. Rev. B* **39**, 9929 (1989).
- ¹²G. A. Garfunkel, G. B. Alers, and M. B. Weissman, *Phys. Rev. B* **41**, 4901 (1990).
- ¹³K. S. Ralls and R. A. Buhrman, *Phys. Rev. Lett.* **60**, 2434 (1988); *Phys. Rev. B* **44**, 5800 (1991); K. S. Ralls, D. C. Ralph, and R. A. Buhrman, *ibid.* **40**, 11 561 (1989).
- ¹⁴N. M. Zimmerman, B. Golding, and W. H. Haemmerle, *Phys. Rev. Lett.* **67**, 1322 (1991); B. Golding, N. M. Zimmerman, and S. N. Coppersmith, *ibid.* **68**, 998 (1992).
- ¹⁵K. Chun and N. O. Birge, *Phys. Rev. B* **48**, 11 500 (1993).
- ¹⁶D. C. Ralph and R. A. Buhrman, *Phys. Rev. B* **51**, 3554 (1994).
- ¹⁷D. Richter, in *Quantum Aspects of Molecular Motion in Solids*, edited by K. Heidemann *et al.*, Springer Proceedings in Physics Vol. 17 (Springer, New York, 1987), pp. 140–152.
- ¹⁸Muon spin relaxation has also been used to study tunneling in insulating crystals; see R. F. Kiefl *et al.*, *Phys. Rev. Lett.* **62**, 792 (1989); R. Kadono *et al.*, *ibid.* **64**, 665 (1990).
- ¹⁹H. Wipf *et al.*, in *Quantum Aspects of Molecular Motion in Solids* (Ref. 17), pp. 140–152 and 153–157; D. Steinbinder *et al.*, *Europhys. Lett.* **6**, 535 (1988).
- ²⁰A. J. Leggett *et al.*, *Rev. Mod. Phys.* **59**, 1 (1987), and references therein.
- ²¹H. Grabert and U. Weiss, *Phys. Rev. Lett.* **54**, 1605 (1985).
- ²²M. P. A. Fisher and A. T. Dorsey, *Phys. Rev. Lett.* **54**, 1609 (1985).
- ²³J. Kondo, *Physica* **124B**, 25 (1984); **125B**, 279 (1984); **126B**, 377 (1984).
- ²⁴K. Yamada, A. Sakurai, and M. Takeshige, *Prog. Theor. Phys.* **70**, 73 (1983).
- ²⁵Y. Kagan and N. V. Prokof'ev, *Zh. Éksp. Teor. Fiz.* **90**, 530 (1985) [*Sov. Phys. JETP* **63**, 1276 (1986)].
- ²⁶A. O. Caldeira and A. J. Leggett, *Ann. Phys. (N.Y.)* **149**, 374 (1983).
- ²⁷S. Chakaravarty and A. J. Leggett, *Phys. Rev. Lett.* **52**, 5 (1984).
- ²⁸K. Chun and N. O. Birge, *Phys. Rev. B* **49**, 2959 (1994).
- ²⁹S. Machlup, *J. Appl. Phys.* **25**, 341 (1954).
- ³⁰B. L. Al'tshuler and B. Z. Spivak, *Pis'ma Zh. Éksp. Teor. Fiz.* **49**, 671 (1989) [*JETP Lett.* **49**, 772 (1989)].
- ³¹A. Yu. Zyuzin and B. Z. Spivak, *Pis'ma Zh. Éksp. Teor. Fiz.* **43**, 185 (1986) [*JETP Lett.* **43**, 234 (1989)].
- ³²M. Faas and B. L. Al'tshuler, *Phys. Rev. B* **48**, 18 043 (1993).
- ³³Zimmerman and co-workers (Ref. 14) made a slightly smaller estimate of $\text{rms}(\varepsilon)$ because they inadvertently used the sample

- length, instead of the thickness, in Eq. (7).
- ³⁴R. I. Cukier, M. Morillo, K. Chun, and N. O. Birge, Phys. Rev. B **51**, 13 767 (1995).
- ³⁵H. Grabert, Phys. Rev. B **46**, 12 753 (1992). (It is not clear to us why the phonon coupling proposed by Grabert contributes so far below the Debye temperature.)
- ³⁶N. O. Birge, B. Golding, and W. H. Haemmerle, Phys. Rev. Lett. **62**, 195 (1989); Phys. Rev. B **42**, 2735 (1990).
- ³⁷P. McConville and N. O. Birge, Phys. Rev. B **47**, 16 667 (1993); J. S. Moon, N. O. Birge, and B. Golding, *ibid.* **53**, R4193 (1996).
- ³⁸See, for example, N. O. Birge, B. Golding, W. H. Haemmerle, H. S. Chen, and J. M. Parsey, Jr., Phys. Rev. B **36**, 7685 (1987), or P. Esquinazi, R. Konig, and F. Pobell, Z. Phys. B **87**, 305 (1992).